RAPID COMMUNICATIONS

PHYSICAL REVIEW A VOLUME 35, NUMBER 6 MARCH 15, 1987

Traveling waves and spatial variation in the convection of a binary mixture

Richard Heinrichs, Guenter Ahlers, and David S. Cannell
Department of Physics, University of California, Santa Barbara, California 93106
(Received 20 October 1986)

We report measurements of heat transport and shadowgraph flow visualizations for a binary mixture with separation ratio $\psi \cong -0.12$. Beyond a Hopf bifurcation from pure conduction, a traveling-wave state involving a single frequency develops and consists of a small number of convection rolls concentrated near the sidewall toward which it is moving. Thus about 60% of our cell is left in the pure conduction state. At a slightly larger Rayleigh number, the traveling wave becomes amplitude modulated by a second, lower frequency.

Much progress has been made in the elucidation of dynamical systems with a small number of relevant degrees of freedom.[1] Recently, therefore, emphasis has been placed on nonlinear nonequilibrium systems with spatial variation, in which the number of degrees of freedom potentially can be much larger.[2] A binary fluid mixture heated from below and undergoing convective motion[3] is an example of a system with interesting dynamical properties involving spatial variation. It has been observed and predicted[4-7] that this motion can consist of convective rolls traveling as waves rather than being stationary in space. Our experiments indicate that these traveling rolls in steady states can be concentrated near one or the other end of a long narrow cell, leaving the remainder without convection. The resulting spatial variation is similar to recent predictions by Cross.[8]

In a pure fluid, the parameters which mainly determine the convective flow are the Rayleigh number R, the Prandtl number σ, and the geometry of the lateral walls. In a two-component mixture there are two additional relevant parameters.[9] One of them is the Lewis number L. The other, the separation ratio ψ, determines whether gradients in the concentration c help or hinder convection. For $\psi > 0$ ($\psi < 0$) concentration gradients destabilize (stabilize) the pure conduction state. The experiments used ethanol-water mixtures and are for $\psi < 0$ where pure conduction loses stability via a Hopf bifucation[9] at a reduced Rayleigh number $r_{co} = R_{co}/R_c^0 > 1$ (R_c^0 is the critical Rayleigh number of a pure fluid). However, the resulting oscillating transients do not lead to nonlinear saturation until rather large amplitudes are reached, even for $r = R/R_c^0$ very close to r_{co}.[4] These long-lived transients were observed by Caldwell,[6] and were studied in considerable detail recently by Kolodner, Passner, Surko, and Walden.[10] In a narrow cell of finite length they consist of the superposition of right- and left-traveling waves which are partly reflected from the cell ends and grow significantly while traversing the cell.[8,10] Our observations are consistent with those results, but our work has concentrated on the late stages of the transients and the final nonlinear steady state of the system. The convection cell had a height $d = 0.308$ cm, a width w such that $L_1 = w/d = 4.87$, and a length l such that $L_2 = l/d = 25.3$. The fluid was 25 wt.% ethanol in water at a mean temperature of 26.0 °C, and had $t_v \equiv d^2/\kappa = 83.6$ sec, $\sigma \cong 18$, $L \cong 0.015$, and $\psi \cong -0.12$. The apparatus[11] enabled us to make high-resolution heat-flow (Nusselt number) measurements and to produce computer-enhanced shadowgraph flow visualizations.

The steady-state Nusselt-number results in Fig. 1 show that there are two or more convective states (similar multistability had been observed by Caldwell[6]). The one represented by filled circles is the *first* nonlinear state reached after the Hopf bifurcation, and thus we studied it, and the nonlinear transients leading to it, in detail. Figure 2 shows computer-enhanced[11] shadowgraph images during the transients which result upon increasing r to slightly (0.2% or so) above r_{co} [Fig. 2(a)–2(d)], and of the steady state Fig. 2(e) represented by the left-most filled circle in Fig. 1. Figure 2(a) has common features with the transients reported by Kolodner *et al.*[10] This is more clearly illustrated in Fig. 3(a), where the shadowgraph signal, averaged over the central 55% of the image in the short direction, is plotted versus position in the long direction at time intervals of $0.12t_v$. The left portion of the cell is dominated by left-traveling waves, whereas the right contains primarily right-traveling waves. Near the center, the superposition yields standing waves. At the late stage of the

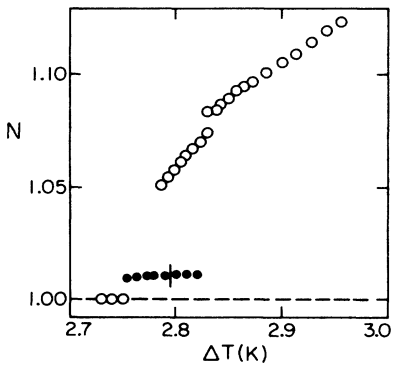

FIG. 1. Steady-state Nusselt numbers as a function of the temperature difference across the cell. The work presented in this paper pertains to the state represented by the filled circles. The data points to the left of the small vertical bar correspond to pure traveling-wave states, and those to the right to amplitude-modulated traveling-wave states.

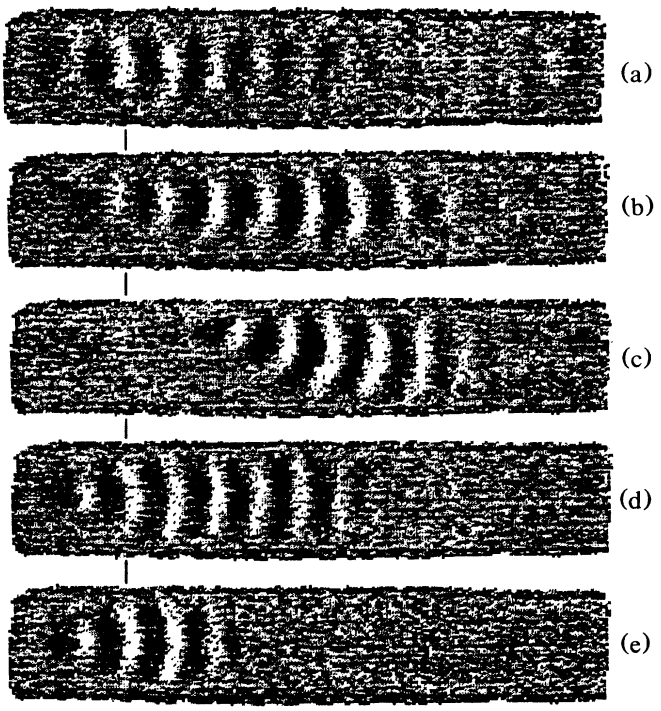

FIG. 2. Computer-enhanced shadowgraph images of the convective pattern during the transients (a)–(d) leading from pure conduction to the convecting state (left-most filled circle in Fig. 1), and of the resulting steady state (e). The images are taken 15, 29, 39, 383, and 1930 vertical diffusion times t_v after the temperature difference was increased by 0.01 K and the conduction state rendered unstable.

transient (compared to the work of Ref. 10), represented by Figs. 2(a) and 3(a), the right-left symmetry of the flow is already broken. A short time later, represented by Figs. 2(b) and 3(b), the right-traveling waves have been nearly expelled from the system, and the flow consists primarily of seven or eight noticeable left-traveling roll pairs surrounded on both ends by nonconvecting fluid. A reduction in the velocity of the waves is noticeable by comparing the slopes of the crests or valleys in Figs. 3(a) and 3(b). This corresponds to a frequency decrease as shown in Fig. 4, where $\omega \equiv 2\pi f t_v$ (with f in Hz), determined at the location indicated by the vertical bars in Fig. 2, is shown as a function of time. The precipitous drop in ω has also been observed by Caldwell,[6] and has similarities to the behavior[12] of the solutions to the eight-mode Lorenz truncation proposed recently[13] by Cross. However, in the model the oscillations decay to zero frequency, whereas in our experiment they persisted at *constant* frequency for the duration of the run ($2000 t_v$) and presumably are a steady state. The late spatial evolution of the traveling-wave pattern is illustrated in Figs. 2(c)–2(e) and 3(c), where 2(e) and 3(c) represent the final steady state. There is no change in the traveling-wave speed beyond the time of Fig. 2(c), but the number of rolls decreases until the convective flow fills only about 30% of the cell, and is located near the narrow sidewall toward which the waves are traveling. The spatial

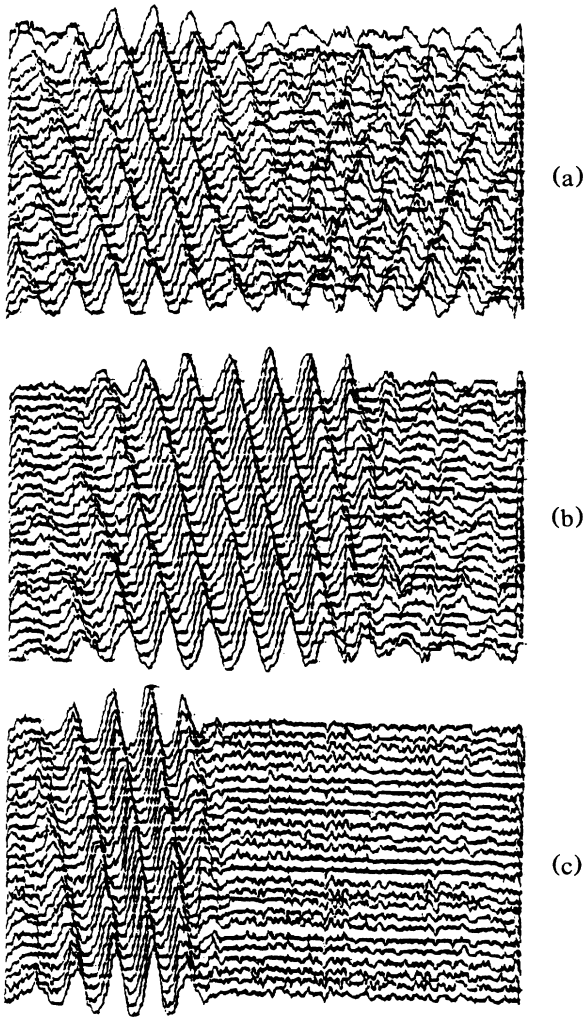

FIG. 3. Contour plots, consisting of shadowgraph signals (averaged over 55% of the cell width) as a function of position along the length of the cell, at time intervals of $0.12 t_v$. Time increases in the upward direction. From left to right, the plots span the entire cell length. They are for nominally (a) $15 t_v$, (b) $29 t_v$, and (c) $1930 t_v$ and may be compared to the images in Figs. 2(a), 2(b), and 2(e), respectively.

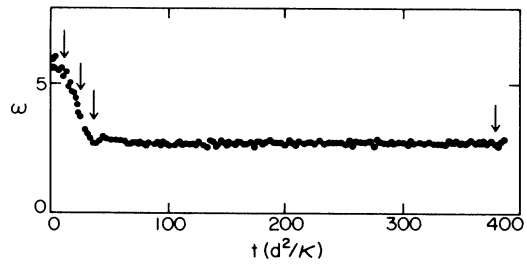

FIG. 4. The frequency of the traveling waves measured with the shadowgraph signal as a function of time at the location indicated in Fig. 2 by the vertical bars between the images. Each point is based on the determination of a single period of the signal. The four arrows correspond to the times of Figs. 2(a)–2(d).

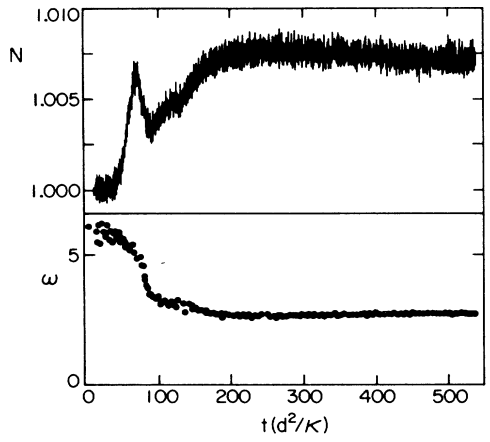

FIG. 5. The evolution of the Nusselt number and the frequency of the traveling waves during the transients from pure conduction to convection.

structure of this state has a qualitative similarity to the prediction by Cross[8] which is represented by the lower half of his figure. A quantitative comparison with the theory has yet to be made.

In order to further characterize the transients, we show in Fig. 5 a comparison (obtained in a separate experimental run) of ω (as in Fig. 4) with the evolution of the Nusselt number. The early stage, during which N increases and ω is nearly constant and close to six, corresponds to the linear growth region.[10] Here ω is close to the theoretically predicted Hopf frequency.[9] When nonlinear effects become important, both N and ω decrease. At a later time, N increases once more while ω becomes nearly steady.

For the steady state, we show in Fig. 6 the Nusselt number and the shadowgraph signal S (obtained at the location indicated in Fig. 2) for the state represented by the filled circle just to the left of the small vertical bar in Fig. 1. The flow pattern is very similar to that shown in Fig. 2(e). The heat transport is not influenced within our resolution by the roll translation which leads to oscillations in S at frequency ω_1. The absolute value of the Fourier transform $\hat{S}$ of S is shown in the bottom part of Fig. 6. It reveals a single spectral component at $\omega_1 \cong 2.66$.

Observations very similar to those for $\psi = -0.12$ have also been made for $\psi = -0.21$. The transients were analogous to those leading to the pattern of Fig. 2(c), but thereafter that pattern and N gradually grew and convective rolls finally filled the entire cell. During this growth the frequency was constant at $\omega_1 \cong 4.4$ and about equal to $\frac{1}{2}$ the frequency of the linear state as in Figs. 4 and 5, but when the cell was completely filled and the trailing end of the traveling rolls touched the sidewall, ω decreased further to about $0.3\omega_1$.

Figure 7 shows data for $\psi = -0.12$ similar to those in Fig. 6, but for the state just to the right of the small vertical bar in Fig. 1. For this case the shadowgraph images still look essentially like Fig. 2(e), but the Nusselt number oscillated at a frequency $\omega_2 = 0.53$, approximately equal to $\frac{1}{5}$ the frequency $\omega_1 = 2.72$ of the traveling waves. While S oscillated at ω_1, its amplitude was modulated at ω_2. The absolute values of the Fourier transforms $\hat{N}$ and $\hat{S}$ of N and S are shown in the lower two portions of Fig. 7. The spectrum of N contains only the modulation frequency ω_2. The spectrum of S is made up entirely of ω_1 and $\omega_1 \pm \omega_2$, indicating amplitude modulation of the waves. Such a modulated traveling-wave state bifurcating from the traveling waves has been predicted by Knobloch.[5] At slightly larger r, the state illustrated in Fig. 7 lost stability.

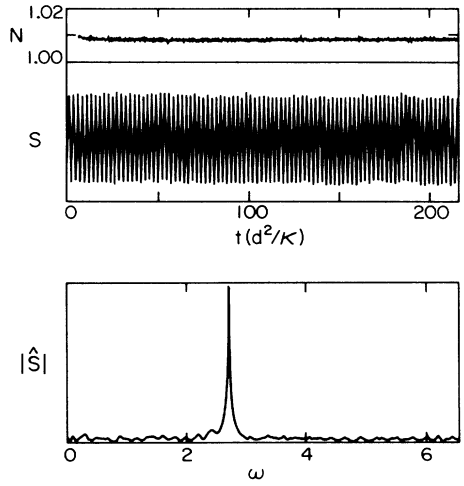

FIG. 6. The Nusselt number N, the shadowgraph signal S at the location indicated in Fig. 2, and the absolute value of the Fourier transform $\hat{S}$ of S for the steady state just to the left of the small vertical bar in Fig. 1.

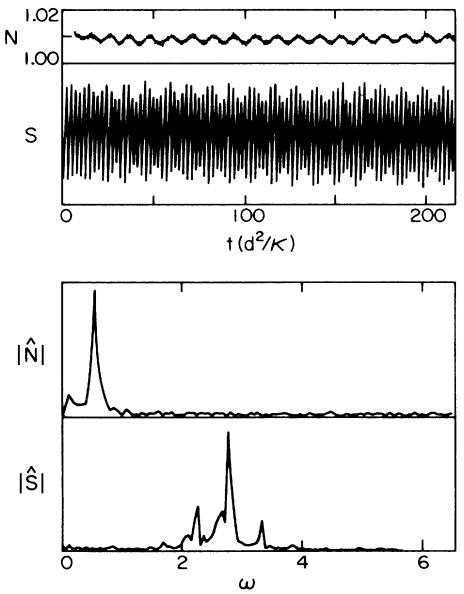

FIG. 7. The Nusselt number N, the shadowgraph signal S at the location indicated in Fig. 2, and the absolute values of the Fourier transforms $\hat{N}$ and $\hat{S}$ of N and S for the steady state just to the right of the small vertical bar in Fig. 1.

Its trailing end moved away from the leading end by the addition of more rolls and N increased. When the trailing end touched the side wall, the frequency ω_1 decreased, as was the case for $\psi = -0.21$. The final state corresponded to the upper branch in Fig. 1.

This work was suppported by National Science Foundation Grant No. MSM85-14917. We are grateful to Christopher Meyer for his help in the software development, and to Bryan Jasper for his help in constructing the apparatus.

[1]For a brief review and a comprehensive set of references, see, for instance, N. B. Abraham, J. P. Gollub, and H. L. Swinney, Physica D **11**, 252 (1984).

[2]See, for instance, the proceedings of the recent conference on spatio-temporal complexity [Physica D (to be published)].

[3]For a review, see, for instance, J. K. Platten and J. C. Legros, *Convection in Liquids* (Springer, New York, 1984), Chap. 9.

[4]C. S. Bretherton and E. A. Spiegel, Phys. Lett. **96A**, 152 (1983); P. Coullete, S. Fauve, and E. Tirapegui, J. Phys. (Paris), Lett. **46**, L787 (1985).

[5]E. Knobloch, Phys. Rev. A **34**, 1538 (1986), and references therein.

[6]To our knowledge, the first experimental evidence for traveling waves (as opposed to standing waves) can be found in the work of D. R. Caldwell, J. Fluid Mech. **64**, 347 (1974), who observed local oscillations at a frequency ω in the fluid temperature and yet found no oscillations in the total heat flux at frequencies near 2ω (oscillations in the heat flux would have been produced by standing waves). The first direct observations of traveling waves by flow visualization were obtained by R. W. Walden, A. Passner, and C. M. Surko, Phys. Rev. Lett. **55**, 496 (1985).

[7]E. Moses and V. Steinberg, Phys. Rev. A **34**, 693 (1986).

[8]M. C. Cross, Phys. Rev. Lett. **57**, 2935 (1986).

[9]D. T. J. Hurle and E. Jakeman, J. Fluid Mech. **47**, 667 (1971); D. Gutkowicz-Krusin, M. A. Collins, and J. Ross, Phys. Fluids **22**, 1443 (1979); **22**, 1451 (1979).

[10]P. Kolodner, A. Passner, C. M. Surko, and R. W. Walden, Phys. Rev. Lett. **56**, 2621 (1986).

[11]V. Steinberg, G. Ahlers, and D. S. Cannell, Phys. Scr. **32**, 534 (1985).

[12]G. Ahlers and M. Lücke, Phys. Rev. A **35**, 470 (1987).

[13]M. C. Cross, Phys. Lett. **119A**, 21 (1986).